Kate Gleason College of Engineering
Rochester Institute of Technology
Rochester, New York 14623

P20652: Medium-scale 3D Concrete Printer

Amiee Jackson, Alex Kelly, Chad tenPas, Nick Claver,
Alexander Pegot-Ogier, Joseph Bragg, Mary McCombs, Seth Deane

Abstract

Currently, 3-dimensional (3D) concrete printers are used to print large-scale structures such as houses. Students of Multidisciplinary Senior Design (MSD) at Rochester Institute of Technology (RIT) do not have an efficient and accurate way to prototype medium-scale concrete objects. A 3D concrete printer was designed that uses a computer-controlled motion system to deposit a prepared mixture of concrete along a planned path in a uniform and controlled flow. Our solution is a custom, stepper motor driven, vertical auger-based extrusion system mounted onto a cartesian motion system and controlled via a Duet 2 Wifi controller board from a local web browser. The XYZ cartesian design is a cube structure design with outside dimensions of 1450mm x 1540mm x 1000mm (Length x Width x Height). Plastic 3D printed parts were utilized to reduce cost. The motion system integrates stepper motors with linear ball screws and rails. Mixture development was limited for simplicity to Sakrete S-type mortar mix. This enables rapid and low cost concrete prototyping for MSD teams at RIT. The delivered product was able to achieve two dimensions of printing. This paper presents the technical design, prototyping process followed, obstacles faced, progress achieved, and future plans for project P20652.

Background And Motivation

A medium-scale 3D concrete printer was designed for future MSD students who need to quickly prototype concrete objects. The motivation for selecting concrete as a printing material was its low cost, availability, flexibility of form, strength, and durability. Past MSD teams have encountered difficulties while creating concrete projects such as arboloos and roof tiles as shown in Figure 1. Difficulties encountered include high costs, lifespan, and manufacturing time. The motivation for this project is to create an alternative solution for those MSD teams that reduces the cost, complexity, and time involved in forming concrete objects.

Figure 1: Current MSD Concrete Manufacturing Processes

Recent research and development into concrete 3D printing generated interest in bringing this technology to RIT. Current printers exist in a variety of coordinate systems with the ability to print a variety of mixtures. At the industrial level, some printers are capable of printing homes faster than traditional construction.

Customer requirements for the printer were specified by the customer. Printed parts should be dimensionally accurate to a target tolerance of 0.5”. Strength of the concrete mixture should be comparable to that of traditional concrete mixtures. All aspects of the machine’s workflow including: programming, mixture loading, operation, cleanup, maintenance, etc. should be intuitive, ergonomic and efficient. The material delivery system should be easy to access for cleaning and maintenance. Set-up and take-down of the machine should be fast and ergonomic. Finally, the machine should be stored in a smaller volume than it occupies at set-up. The starting budget for the project was $1500 for delivery in May 2020.

Description Of Design

The design process began by selecting a motion system (cartesian, coreXY, or delta). A cartesian system was selected due to its popularity and simplicity. The final design uses a cube structure to improve rigidity and prevent binding in stepper motors. The final CAD model is shown in Figure 2.

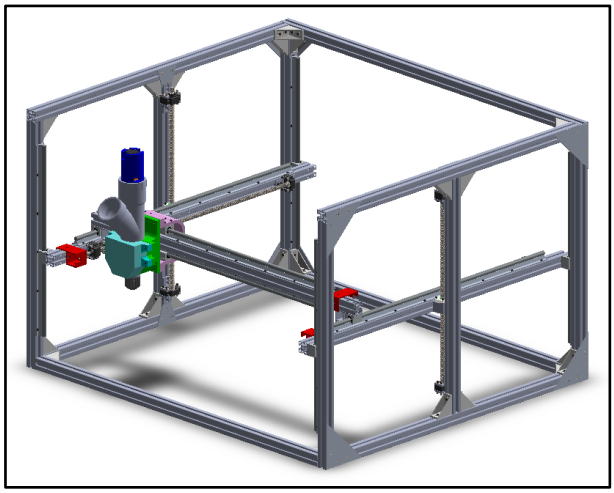

Figure 2: Finalized CAD Model

In-House Design

Iterative 3D printing with polylactic acid (PLA) material was integral to our design and was used for several components in the final design. Metal fabrication was used to create brackets for the final design. 3D printed and metal prototyped designs are discussed below.

PVC Wye

A Charlotte Pipe 3” PVC wye was repurposed as an extrusion manifold. A threaded adapter was spliced from a 3” diameter to 1 ½” diameter and added to the bottom section of the wye where threaded nozzle attachments can be utilized to achieve different extrusion geometries. The PVC wye was selected for its workability with 3D plastic printing for internal components such as the auger and plastic bearings. See Figure 3.

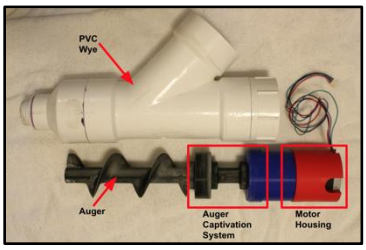

Figure 3: PVC Wye, Auger, and Stepper Motor in Housing

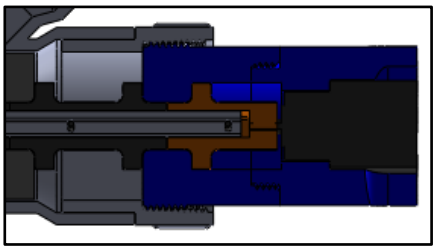

Figure 4: Cross-section view of Extruder Motor Housing and ACS

Auger Captivation System

The auger captivation system (ACS) was formulated after early concrete extrusion tests that showed the auger rising out of the PVC wye. The ACS constrained the auger to the PVC wye and allowed the auger to provide a continuous axial force to the concrete. The ACS is shown in Figure 3 and Figure 4. The ACS threads into the PVC wye to keep the auger in place. The black disk at the top of the auger keeps the system stable and centered in the PVC wye to minimize radial wobble.

Auger

The auger was printed five times with improvements between each iteration as shown in Figure 5. The first prototype was constructed to fit the PVC wye extruder housing snugly with rounded blade edges. Auger binding and mechanical wear was caused by the rounded blade edges and tight fit. In later iterations, the radius of the auger was decreased to allow for more space between the auger and the PVC wye. The auger blade was sharpened to reduce concrete friction between the auger blades and PVC wye.

Figure 5: Auger Progression

Extrusion Nozzles

The PVC extruder housing has threads at the bottom of the extruder to allow different nozzle shapes and sizes to be easily swapped. A 0.5” square and a 0.5” diameter circle have been 3D printed as shown in Figure 6 and Figure 7. The 0.5” dimension was selected based on the customer requirement constraining minimum feature size to 0.5”. Using our custom mixture of S-type mortar mix, extrusion was rarely successful through such small nozzles. Successful extrusion was majorly achieved without the attachment of a nozzle, only using the 1 0.5” threaded adapter as a nozzle.

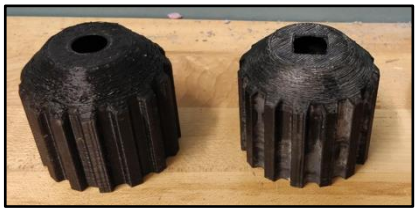

Figure 7: Examples of the 2 Nozzle Geometries

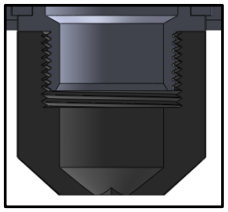

Figure 6: Section view of the extruders nozzle.

Extruder Mount

The 3D printed PVC wye mount attaches the concrete extruder assembly to the linear rails while providing ease of access for assembly, disassembly, and maintenance. A major concern for the mount is the weight of the extruder assembly itself which generates a moment about the X-axis. To prevent bowing of the ballscrew, the forces from this moment are transferred instead to the linear rails, thus maintaining the extrusion assembly in a vertical position. The extruder mount is shown in Figure 8 and Figure 9.

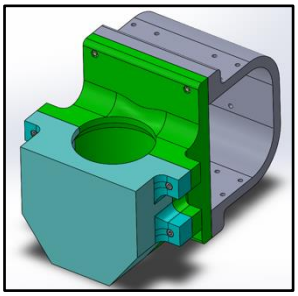

Figure 8: Extruder Mount Alone

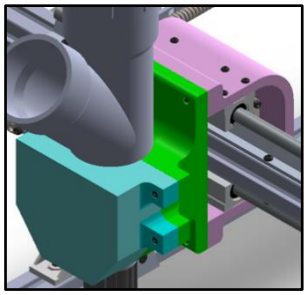

Figure 9: Extruder Mount in Printer

Metal Fabrication by the RIT Machine Shop

Ball screw support block brackets that mount the ball screw blocks to the aluminum extrusion frame, as shown in Figure 10, were designed and machined from L-channel by the RIT machine shop.

Custom X-Y mount brackets to mount the X-axis to the Y-axis were designed, machined and welded in house out of 5052 aluminum alloy as shown in Figure 11.

The structural support plates were designed to aid in perpendicularity of the structure. There are two configurations: corner plate as shown in Figure 12 and side plate shown in Figure 13.

Figure 10: Ball Screw Support Block Bracket

Figure 11: X-Y mount.

Figure 12: Corner Support

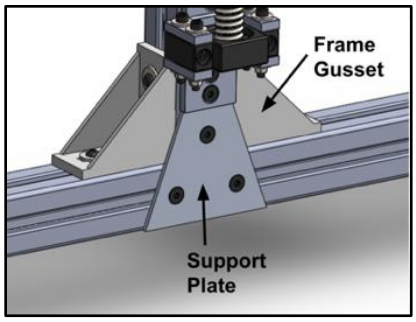

Figure 13: Z-Axis, Z-motor Support and Frame Gusset

Component Selection

Complex components that could not be created in-house were sourced. Additionally, if a product was too costly to purchase, the commercially available design was 3D printed with credit given to the designer.

Frame Gussets

In order to ensure perpendicularity within the 80/20 extruded aluminum structure, gussets are used at each joint. These items were originally sourced from 80/20 [1], but to reduce cost, they were 3D printed with PLA plastic at 100% infill. Frame gussets are shown in Figure 13.

Linear Rail

Due to the scale of the machine and the loads it is designed to translate, linear rails were critical to reduce vibrations and redirect radial loads from the ball screw. Linear rail selection was based off of benchmarking other CNC machines, price, and availability.

Aluminum Extrusion

Aluminum extrusion was used for the structural frame. Due to a conservative bending analysis performed by the team, deflection calculated with the 45x45 standard profile was deemed sufficiently small and was selected.

Ball Screw

To convert rotational motion of the stepper motors into translational motion, C7 grade carbon steel, rolled-thread ball screws were used with a 5mm lead. Selection criteria was based mainly on length, availability and price. Screw diameters in X and Y are 16mm, and 20mm in Z due to the greater load on the system in the Z axis. A conservative buckling analysis for the Z-axis screws led to the diameter increase decision. The maximum recommended dynamic load for the 16mm diameter screws is 1526N, while for the 20mm diameter screws is 1938N. Thanks to the small lead, the ball screws are self-locking [2] and provide motion accuracy well beyond what is required for the machine at 50um/300mm. The critical shaft speed of the 16mm diameter screws is approximately 2500RPM, while for the 20mm diameter is over 3000RPM [3]. This translates to a maximum linear velocity of the motion system of 200mm/min and 250mm/sec, respectively. The capabilities afforded the machine by these specifications were deemed satisfactory and beyond the requirements of machine performance.

Power Supply

There are three main aspects that were considered in the PSU selection: voltage, current, and power. The operating voltage, max current draw, and power consumption ratings for each component helped to generate the system requirements. They were as follows: connectable to a wide variety of systems, supply a minimum of 100 (W) and potentially 200 (W), supply a minimum of 15 (A) current draw, able to source from a wall outlet of ~120 (VAC), at least one 24 (V) output, and general protections such as: overload, over voltage, and, over temperature. PSU models were compared to additional factors such as cost, safety and special features. Our selection of the MeanWell LRS-350-24 [4] provides for a large safety margin that may be useful for future additions of more demanding components.

Stepper Motor

Motor selection was based on three main categories: power supply capabilities, application environment and performance specifications. Each category contained selection requirements.

- **Power Supply Capabilities**: supply voltage available, peak and operating voltage/current outputs of the stepper drivers.
- **Application Environment**: max weight allowable (of the motor) and the maximum dimensions allowable (of the motor).
- **Performance Specifications**: rated torque, holding torque, stall torque, detent torque limits, and torque-speed characteristics.

A list of motors was generated that met these requirements. Then, project constraints such as budget, availability, and outlying purchasing conflicts were considered.

A Permanent-Magnet DC Motor simulation was modeled in MATLAB and Simulink to model stepper motor functionality. The theory for the model used is described by Lyshevski [5] and Umans [6]. The implementation of the model was guided by Morar [7], Le-Huy [8] and MathWorks[9]. The results tracked phase voltages, phase currents, electromagnetic torque, angular velocity, and angular displacement versus time. This simulation provided insight to operational characteristics for the specific motors considered for our selection, in the environment that our PSU and control board would provide.

The selection process led us to select a NEMA 17 single stack stepper motor with relatively high phase current [10] for the axes, and a 5.18:1 Geared NEMA 17 stepper motor for the auger. Eventually, this decision was rescinded and determined that a NEMA 23 should be tested. The geared motor would stall because it was required to produce torque that, due to the 5.18:1 gear ratio, could not be met by the motor at the desired operating speed. The progress of the project was halted before we were able to test other motors for the extrusion system.

Emergency Stop (E-Stop)

The E-Stop is a highly visible button that will immediately disconnect motors from the power supply for emergency situations. The "stop" functions are described by 3 categories [11]. The determined functionality for our project was Category 0: an uncontrolled stop by immediately removing power to the machine actuators. Activation of the stop shall entirely prevent the actuators from being energized (as quickly as possible without creating any additional hazard) without a deliberate, mechanical reset. These safety requirements were easily met using a push-button, normally closed, emergency stop switch that remains cutoff after activation.

Control Board

After benchmarking other 3D concrete printers, it was apparent that Duet 3D was the most popular choice of control board. In addition to benchmarking, this control board was selected for its high quality stepper motor drivers, vast motor expandability, and friendly included user interface. The company (Duet3D) graciously donated a Duet 2 Wifi control board and Duex 5 expansion board.

Mixture Development

The main focus of the project was on building the printer rather than developing the ideal mixture. However, not just any mixture of cement, water, aggregate, and admixture can be used. To narrow the design space, we selected Sakrete S-Type mortar mix as the base of the mixture, and only varied the water to mortar (W:M) ratio in our development and specification. To specify the mixture, the standard slump test [12] was modified as shown in Figure 14. The slump cone geometry was reduced by approximately 50%, then multiple iterations of mixtures across the design space were tested. This was done to identify over what range of slump values our ideal mixture could be specified with the modified cone. A measured slump of approximately 2.5-4cm was regarded as ideal, achieved with a W:M ratio of 0.25.

Figure 14: Slump Cone During Testing

Another major criteria for mixture selection is the setting time, or the time required until one bead can support at least another on top of it. A characterization of setting time for three mixtures using a Brainard Kilman S-170 pocket penetrometer was attempted. However, the useful conclusions from this testing were that the mixture does not need to be set to the extent that the pocket penetrometer measures. That is, qualitative observations indicated a less-set mixture than what was measurable with the pocket penetrometer could support layers above it.

To determine the mortar weight and water volume necessary to achieve a specific W:M ratio, we developed a spreadsheet calculator. The basis for the calculator was backwards approximation of the mortar's density using input-to-output estimations provided by the manufacturer. An estimated density of 2.44 g/cc was adequate for the purpose of making several liters of mixture per batch. Then, water volume was determined by multiplying the desired W:M ratio with the desired volume of mixture, and mortar weight was determined by multiplying the difference between desired volume of mixture and water volume required with the mortar density.

The amount of each component included in the mixture is not the only consideration to developing an adequate mixture. The mixing procedure is important for obtaining between-batch consistency. The procedure we developed was based on traditional mortar mixing techniques and adapted to be performed with the tools and equipment available. It was based around using a hand-mixer at various speeds and takes about 5 minutes to perform.

An idealized matlab model of the extrusion assembly geometry was used to predict the relationship between auger angular velocity and the outlet flow rate of mortar. It should be noted that this model is rudimentary and includes many unrealistic assumptions regarding the shear behavior of the mortar mix.

SUPPORTING FEASIBILITY EVIDENCE

While hours of thought were put into component selection and design, it is important to prove that these selection efforts were feasible.

Subsystem Testing

After the design and selection process, each subsystem was tested. Additionally, the full system was tested at the point at which it was completed in two dimensions.

Extrusion Subsystem

The extrusion subsystem (including PVC wye, auger captivation system (ACS), the auger, the extruder motor housing, and geared NEMA 17 motor) was tested independently. Various milestones were documented to prove extrusion subsystem functionality. The first milestone was to prove the auger could move smoothly in the PVC Wye without concrete. Sanding the outside edges of the auger was needed. After deciding on an auger design, concrete was added. The second milestone was to print a single layer bead using a wooden rig with and motorized extruder while the X axis was controlled by hand. The third milestone was to print several stacked layers of beads with the motorized extruder and X axis. All milestones were achieved as shown in Figure 15, Figure 16 and Figure 17 below.

Figure 15: First Milestone

Figure 16: Second Milestone

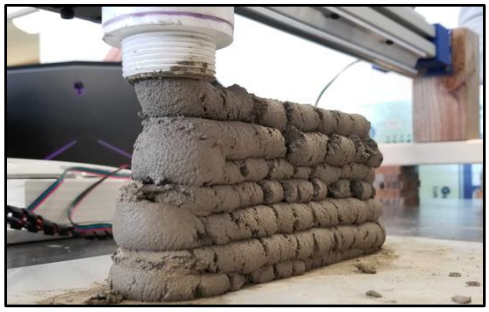

Figure 17: Third Milestone

Structure Subsystem

The structure subsystem consisted of the 80/20 framing, gussets, and connecting mechanisms. The 80/20 framing was solid enough to provide a mechanically rigid structure. The gussets were 3D printed in order to reduce costs. These 3D printed gussets have not been tested as a reliable means of holding the structure square.

During the 2D build, a temporary structure was built out of wood in order to test the motion subsystem. The temporary structure was not built using gussets and was admittedly not perfect. Because of this temporary setup, some binding was present when moving the Y axis motors and ball screws. When the Z dimension is completed, binding should be further reduced due to the added rigidity of the cube structure and the elimination of temporary wooden components.

Motion Subsystem

The motion subsystem included the power distribution, Duet 2 Wifi, motors, ball screws, and linear rails.

Testing power distribution consisted of connecting and operating each circuit independently. The following schematic in Figure 18 shows how the electrical system is connected. The power distribution system includes the power supply unit (PSU), the emergency stop (E-Stop) relay, the microcontroller (Duet 2 Wifi), six motors, and three limit-switches. The PSU supplies 24VDC and up to 350W to the Duet 2 Wifi, which then supplies all of the peripheral devices. The power distribution was tested successfully when all motors were able to be run under load simultaneously. The E-Stop was tested successfully when all motors were deenergized instantaneously.

The Duet 2 Wifi board was tested by achieving the following milestones. The first milestone was to connect to the Duet 2 board. The second milestone was to control motors via a web browser. The third milestone was to move the motors with dimensional accuracy by calibrating the number of steps the stepper motor needed to move a certain distance. Finally, the fourth milestone was being able to load and execute a sliced STL model using our own slicer settings.

The motors were tested with a spring scale capable of up to 110 lbs of spring resistance. The motor rotated the ball screw which stretched the spring scale. The NEMA 17, Geared NEMA

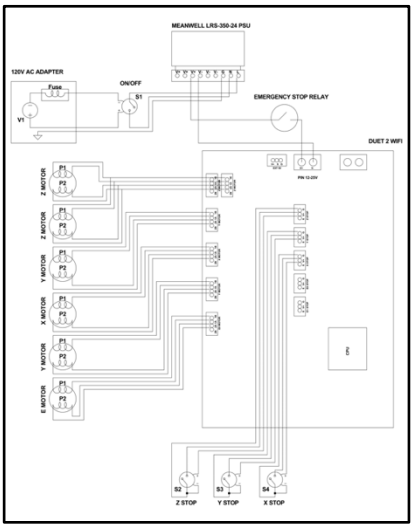

Figure 18: Electrical System Schematic

17, and NEMA 23 motors were set up with different currents and speeds which impact the torque of stepper motors. This testing proved that the geared NEMA 17 provided the most torque under low speed operation while the ungeared motors provided more torque under high speed operation. The mass scale did not allow for driving the motor at a constant load over an extended period of time. The geared NEMA 17 could not produce enough torque at high rotational speeds due to the 5.18:1 gear ratio for it to be useful as a X or Y axis motor. From all motor testing, it was decided that the geared NEMA 17 would be used for the extruder and Z axis. The NEMA 17 would be sufficient for the X and Y axes. More testing of NEMA 23 motors would be helpful to determine if they would be suitable for the extruder motor or other axes.

The ball screws and linear rails were installed and moved the extruder under load in 2 dimensions without incident.

Full system testing

Due to the impact of the COVID-19 events, printer testing was altered. Focus shifted to ensuring that prints would be dimensionally accurate in the X and Y planes, and that the path of multiple layers would be correct. Except for incorporating extrusion, this activity tested the interactions of each subsystem. Using a blinking LED and remote camera shutter, we captured long exposure images of the printer completing a path generated in Cura as seen in Figure 19. We also used a marker and whiteboard to trace the path as shown in Figure 20. The user workflow for the machine was further developed, following the design, slice, and print industry standard. Templates of machine, material, and printing profiles for Cura were created for our machine and process. The results supported the validity of the motion and structure subsystem designs and their robustness, while highlighting areas requiring improvement in the bulleted list below.

- Although the printer is constructed with high-velocity and high-performance components, the resulting ability of the printer may not be on the same order of magnitude. Axis binding became an issue because of several potential reasons including: misalignment, over-constraint, motor responsiveness, and mounting solution.
- The X-Y axes mounting brackets may require re-work or replacement.
- Consistent lubrication of the motion components is critical.
- The performance is highly related to the assembly procedure for integrating the axes. See our website for more detailed information:
    - https://edge.rit.edu/edge/P20652/public/Integrated%20System%20Build%20%26%20Test

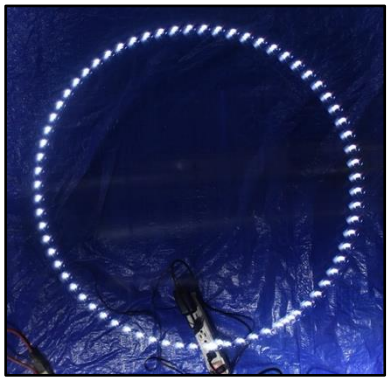

Figure 19: Long Exposure Image of Circular Path

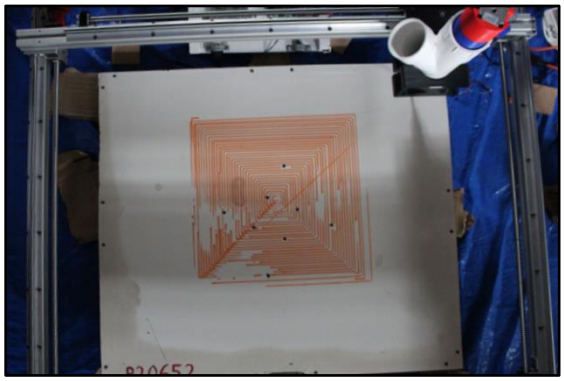

Figure 20: Marker Drawing of 2D Pyramid

The results of analyzing the performance of the marker test conclude that variation between actual and theoretical positioning is low. In fact, the marker drawing did not provide enough resolution to realize an observable variation, so for the example provided below the deviation was 0mm. It is possible that the experiment could be redesigned to generate a physical "read-out" with greater resolution than the marker. However for the scope of this project, sub-millimetre accuracy is not necessary to meet the engineering requirements. To extract the results from the test the theoretical positions for a movement (from the G-code) were compared to actual measurements of the position as recorded by the marker. For example, layers 31 and 32 of the pyramid path should be 30mm and 15mm squares according to the G-code file (segments below.) Confirming the physical dimensions of those layers, the error is 0mm with a ruler.

We did observe some shortcomings to this test besides low resolution. There is enough vibration in the system to induce some "wobble" to the tip, capturing the small but noticeable vibrations in a measurable form. With a higher resolution capturing mechanism, this would increase the scope of the test, however the large tip dry-erase marker does not provide that. Additionally, it was difficult to minimize error in the difference between the levelness of the print head, marker tip, and print bed. While the test is limited by its resolution, it confirms the feasibility of the visual-reference style accuracy tests, it provides proof that the printer is meeting engineering requirements related to positional accuracy and dimensional variation, and it serves as a baseline test to improve reliability and scope.

RESULTS, CONCLUSION, AND RECOMMENDATIONS

On March 11th, RIT closed due to COVID-19 with the remainder of the semester to continue online. This eliminated MSD team's ability to order parts and collaborate in person. At the point of the closure, the X and Y axes had been prototyped. The Engineering Requirements (ER) were addressed as shown in Table 1 where green shows a well addressed ER and red shows a poorly addressed ER.

Table 1: Engineering Requirement Statuses

ER #	Category	Requirement Description (metric)
ER1	Process Time	Setup time
ER2	Process Time	Minimum deposition rate
ER3	Process Time	Minimum time from print finish to remove print from printer
ER4	Process Time	Takedown time
ER5	Process Time	Cleaning procedure time
ER6	Print Quality	% variation in critical dimensions from design to print
ER7	Machine	Minimum feature size
ER8	Material	Maximum Size Aggregate (MSA)
ER9	Print Quality	% variation from planar surface test printed part
ER10	Process Time	Average time to train new user on setup, operation, takedown and cleanup
ER11	Material	Compressive strength of standard size test printed part
ER12	Material	Tensile strength of standard size test printed part
ER13	Machine	Compatible operating systems
ER14	Machine	Compatible model file types
ER15	Machine Size	Printable envelope radius
ER16	Machine Size	Printable envelope height
ER17	Machine Size	Operational Volume
ER18	Machine Size	Storage Volume
ER19	Safety	Industry standard machine safety systems in place
ER20	Safety	MSDS included in documentation
ER21	Cost	Mixture cost per unit volume
ER22	Cost	Machine parts cost (total)
ER23	Machine	Power requirements
ER24	Safety	REBA score for selected tasks of set-up
ER25	Safety	REBA score for selected tasks of operation
ER26	Safety	REBA score for selected tasks of clean-up
ER27	Safety	REBA score for selected tasks of take down

Our experience from the design and prototype has granted us a unique perspective on the current state of the project and project continuation, as well as the ability to provide advice to future teams working on this concrete printer. The most important lessons from both our progress and shortcomings can be adequately summarized in the bulleted list below.

- Process times were not formally measured, although approximate times from team experience and testing can inform the expected range. Material testing for setting time intended to factor into both ER2 and 3, while experience from the material development for ER5 indicates that this requirement would have been passed. ER1 and 4 were untested due to prototyping being cut short.
- We failed to test the extrusion system to the point where we could adequately measure the extrusion flow rate, and therefore determine an estimation for print time based on volume. However, idealized predictions of flow through the extruder were performed, which can be modified and improved with additional mixture and extruder testing to address ER2.
- Due to time constraints, we failed to develop the mixture to the point where we can effectively test the concrete for compression and tension strengths for ER11 and 12. Due to our mortar selection and extruder assembly design, the MSA does not meet ER8. Without testing extrusion in 2 or more axes to print test parts, ER7 and 9 cannot be verified. However, testing in 2 dimensions showed ER6 was met.
- ER13, 14, 19, 20, and 23 were all met by design.
- All machine size requirements, except ER15 were met, where ER15 was marginally met.
- Cost requirements ER21 and 22 were met.
- Ergonomics requirements, ER24, 25, 26 and 27, were not considered due to shortened prototyping.

- Auger prototypes were printed with updates being made between each version. The first prototype was constructed to fit the WYE shaped PVC extruder housing snugly. The first prototype was not able to smoothly extrude concrete because there was too much friction between the auger and the PVC extruder housing. In later iterations, the radius of the auger was decreased to allow for more space between the auger and the PVC extruder housing. Taking an extra look into engineering tolerances, could have avoided this issue.
- In motor selection, we failed to adequately produce a model that could account for the complexities involved with using a motor coupled to a gearbox. Although a gearbox provides the advantage of torque/speed output manipulation, without a predictive model we resorted to physical testing of a geared stepper motor. This is not a thorough or efficient method to assess the validity of motor selection. It is recommended that a future team develops a method to theoretically assess the performance of a geared stepper motor so as to not exclude them as a potential solution.
- Shortcomings in developing the auger geometry and mixture parameters resulted in the inability to create an accurate Cura profile.
- The project would greatly benefit from having a civil or chemical engineer on the team. Someone with above-average knowledge of concrete should be dedicated to the research and prototype a concrete mixture specifically designed to work with our extrusion system.
- Additionally, either the mixture or the extrusion system could form the motivation for a separate project focused specifically on the design of those components and their integration to our printer.

REFERENCES

[1] 80/20. 45 Series 4 Hole - Inside Corner Bracket with Dual Support. https://8020.net/14102.html. [Accessed: 21 April 2020]

[2] Shigley. *Shigley's Mechanical Engineering Design*. New York: McGraw-Hill, 2011. Print.

[3] AluFlexGroup. *Ball Screws Reference Catalog* [Online]. Available: https://www.testwebben.se/6668/Filer/PDF-Kataloger/PDF-Katalog%20Ballscrews.pdf. [Accessed: 21 April 2020]

[4] Mean Well, Wugu Dist., New Taipei City, Taiwan. *LRS-350-SPEC.* [Online]. Available: https://www.meanwell.com/webapp/product/search.aspx?prod=LRS-350 [Accessed: November 2019]

[5] S. E. Lyshevski, *Mechatronics and Control of Electromechanical Systems*, CRC Press, FL, 2017.

[6] Stephen D. Umans, Fitzgerald & Kingsley's *Electric Machinery 7th Edition*, McGraw-Hill, NY, 2014.

[7] A Morar. *The modelling and simulation of bipolar hybrid stepper motor by Matlab/Simulink. Presented at INTER-ENG 2014*. [Online]. Available: https://www.sciencedirect.com/science/article/pii/S2212017315000833. [Accessed: 21 April 2020]

[8] H. Le-Huy. *Stepper Motor Drive*. The MathWorks, Inc. https://www.mathworks.com/help/physmod/sps/examples/stepper-motor-drive.html. [Accessed: November 2019]

[9] The MathWorks, Inc., Natick, MA, US. *Stepper Motor with Control*. Accessed: Nov. 2019. [Online]. Available: https://www.mathworks.com/help/physmod/sps/examples/stepper-motor-with-control.html [Accessed: 21 April 2020]

[10] OYOSTEPPER, Houston, Texas, US. *Stepper Motor 23HS22-2804S*. [Online]. Available: https://www.oyostepper.com/images/upload/File/23HS22-2804S.pdf. [Accessed: November 2019]

[11] NFPA. *Electrical Standard for Industrial Machinery*, NFPA Standard 79, 2018. [Online]. Available: https://www.nfpa.org/codes-and-standards/all-codes-and-standards/list-of-codes-and-standards/detail?code=79. [Accessed: 21 April 2020]

[12] ASTM International. *C143/C143M-15a Standard Test Method for Slump of Hydraulic-Cement Concrete* [Online]. West Conshohocken, PA; ASTM International, 2015 [Online]. Available: https://compass-astm-org.ezproxy.rit.edu/download/C143C143M.18447.pdf. [Accessed: 21 April 2020].

ACKNOWLEDGEMENTS

RIT provided initial funding of $1500 towards the project with an additional $400 increase during phase two of MSD II. Duet 3D donated the Duet 2 Wifi and Duex 5 Expansion Board. 3D-Fuel donated 5 spools of PLA filament (2 spools of "Standard PLA", 2 spools of "Workday PLA", and 1 spool of "Pro PLA"). Manitou Concrete donated concrete supplies (1 five gallon bucket of concrete mix and 1 five gallon bucket of fly ash). The RIT SOIL Lab provided a work space to mix concrete. A special thanks is paid to Teresa Wolcott for setting up the relationship with the RIT SOIL Lab. Thank you to Jan Maneti (Dept. of ME) for providing our team a place to operate and store the printer. Finally, we would like to thank the MSD office for their support throughout the project.